Adaptive Red Panda Optimization for Feature Extraction in Diabetic Retinopathy Detection Using Deep Learning

Mahesh Ramakrishnappa
Nagarjuna College of Engineering and Technology
Visvesvaraya Technological University, India
mahesathya@gmail.com

Rohith Shivashankar
Nagarjuna College of Engineering and Technology
Visvesvaraya Technological University, India
rohithvjp2006@gmail.com

Abstract: *Diabetic Retinopathy (DR) is a diabetes-related eye disease that affects the light-sensitive tissue of the retina and can lead to vision loss if not detected early. Traditional diagnostic approaches often overlook the value of ophthalmic imaging and are typically time-consuming and costly. In this study, we propose an Adaptive Red Panda Optimization-based Deep Convolutional Neural Network (ARPO-based DCNN) for effective DR detection. The methodology involves preprocessing retinal fundus images with a median filter, segmenting lesions using U-Net, and utilizing both the segmented and original images as input to a DCNN, which is trained with the ARPO algorithm-a combination of Red Panda Optimization (RPO) and adaptive mechanisms. For robust evaluation, we employed the publicly available Indian Diabetic Retinopathy image Dataset (IDRiD), which comprises high-resolution, annotated fundus images representing various stages and lesion types of DR, making it a standard benchmark in the field. Experimental results demonstrate that our ARPO-based DCNN achieves superior diagnostic performance, attaining an accuracy of 90.582%, sensitivity of 92.016%, and specificity of 90.272%, thereby highlighting its potential for reliable and automated DR screening.*

Keywords: *Diabetes, diabetic retinopathy detection, convolutional neural network, U-net, red panda optimization.*

Received January 17, 2025; accepted July 10, 2025
https://doi.org/10.34028/iajit/22/5/12

1. Introduction

In recent years, diabetes has become a prevalent health condition affecting individuals worldwide, characterized by elevated levels of glucose in the blood. Diabetic Retinopathy (DR) significantly impacts the financial well-being of society, particularly within the healthcare monitoring system. Prolonged exposure to high glucose levels in the blood vessels leads to persistent damage to the blood vessels. Early discovery of DR is critical for moderating the loss of vision among diabetic individuals. Present strategies aid the patients with inadequate diabetes ought to be calculated for DR every year and the diabetes is controlled by the frequent check-ups [1]. Primarily, DRis differentiated into proliferative and non-proliferative DR wherein, Proliferative DR is caused by the abnormal enlargement of vessels in the eye and leads to strike the circulation of blood [14, 5]. Likewise, the improper expansion of these vessels causes Non-Proliferative Diabetic Retinopathy (NDPR) [3]. Fundus image-based scanning has been emerged as a superior tool for DR diagnosis in its early stages. Regular screening for DR in individuals with long term diabetes is crucial for minimizing the risk of vision loss and slowing down the disease progression [4]. Owing to the sympathetic scenery of DR illness, fundus imaging is more preferred for early-stage screening [10]. The fundus image reveals different retinal structures of the eye [3, 4].

The rapid advancements of imaging schemes offer timely screening and diagnosis for individuals with DR. The psychoanalysis of micro-vascular lesions is an imperative idea of early treatment. In retinal images, classic indications of DR include Hemorrhages (HEs), Micro Aneurysms (MAs), as well as hard and soft exudates are the key lesions in the retinal surface [33]. Recently, Deep learning (DL) has achieved more attraction in diverse of technical appliances, such as semantic understanding and image recognition, and has been utilized for the characterization of DR in the earlier period. The feature learning for DR classification leveraged DL techniques for automatic characterization [30]. Specifically, Deep Convolutional Neural Network (DCNN) efficiently performed automated depiction of fundus photography due to its wider applicability in various recognition tasks. The utilization of Convolutional Neural Network (CNN) structure for image categorization has fascinated by various researchers for the segmentation of blood vessels [1]. DL based detection models are assisted in the risk stratification and early detection of DR, make appropriate interference and preventing loss of sight. Through the automation of the early screening process, DL algorithm reduces the burden in healthcare applications, particularly in area with limited number of ophthalmologists. Moreover, the implementation of DL

technologies for the automatic detection of DR holds promising functionalities for enhancing outcomes of individuals and moderates the global burden of blindness [27].

The primary goal of this paper is to present an Adaptive Red Panda Optimization-based (ARPO) DCNN for DR detection. Here, the median filter is used to pre-process the input fundus image. After that, lesions are segmented by utilizing U-Net. Finally, DR detection is conducted through DCNN by considering segmented image and the input image as input. Here, DCNN is trained with ARPO.

The primary objective of this study is to present an Adaptive Red Panda Optimization-based Deep Convolutional Neural Network (ARPO-based DCNN) for DR detection. The main contributions of this work are summarized as follows:

- Development of a novel ARPO-based DCNN framework: an ARPO-based DCNN is introduced for automated detection of DR from retinal fundus images.
- Integration of U-Net for lesion segmentation: the framework incorporates U-Net for precise segmentation of retinal lesions, thereby enhancing feature extraction and improving the accuracy of DR detection.
- Optimization with ARPO: the DCNN is trained using the ARPO algorithm, which combines Red Panda Optimization (RPO) with adaptive mechanisms to achieve improved convergence and classification performance.
- Comprehensive evaluation on a benchmark dataset: the proposed method is rigorously evaluated using the publicly available Indian Diabetic Retinopathy image Dataset (IDRiD), demonstrating superior accuracy, sensitivity, and specificity compared to existing approaches.

The finest part of this article is listed as: In section 2, the review of diverse conventional approaches related to DR screening is presented. Section 3 derives the ARPO-based DCNN with mathematical modelling. Section 4 deliberates the accomplishments of developed approach and the conclusion and further development of the ARPO-based DCNN is discussed in section 5.

2. Motivation

DR is a significant difficulty of diabetes that leads to visual impairments. It occurs due to the expansion of cracks and leak of blood in the retinal region. Therefore, early-stage screening of DR is vital in preventing individuals from experiencing loss of vision.

2.1. Literature Review

Bansode *et al*. [2] designed a Shark Smell-Jaya Optimization (SS-JO) algorithm for enhanced DR detection. The method had an ability to detect the DR accurately and it efficiently performed blood vessels segmentation. Moreover, this approach failed to employ ensemble-based learning module for improving the effectiveness of the system. Mujeeb Rahman *et al*. [15] designed a Deep Neural Network (DNN) for Automatic Screening of DR. The model produced accurate detection with reduced time and cost. But the model neglected to deploy user-friendly DR classifier for home treatment. Al-Omaisi *et al*. [1] introduced a ResNet-101 for early DR recognition. The method conducted automated screening of DR and enabled earlier and more efficient analysis for big database. Moreover, it did not consider more CNN layers to categorize and detect DR at real time. Bilal *et al*. [3] invented a Visual Geometry Group Network (VGGNet) for automatic screening of DR. The model was employed in clinical applications and accurately differentiated different stages of retinopathy and abnormalities. Moreover, this scheme failed to detect other retinal illness, like cataract and glaucoma. Table 1 shows comparison of traditional approaches on Diabetic Retinopathy Detection (DRD).

Several optimization algorithms have been utilized in the context of DR detection and related medical image analysis tasks, including Particle Swarm Optimization (PSO), Genetic Algorithms (GA), and Artificial Bee Colony (ABC). These techniques have demonstrated effectiveness in global search and feature selection; however, they are often limited by issues such as premature convergence, sensitivity to parameter settings, and suboptimal performance in high-dimensional or complex search spaces. More recently, RPO has been introduced as a nature-inspired approach that improves the balance between exploration and exploitation, but it can still face challenges in adaptability and convergence speed. The ARPO method, as introduced in this study, extends the RPO framework by incorporating adaptive mechanisms that dynamically adjust search strategies according to the problem landscape. This adaptation enhances convergence rates, robustness, and classification performance, making ARPO more suitable for training DL models in DR detection compared to previous optimization approaches.

2.2. Major Challenges

The major issues faced by the existing DR detection techniques is listed below,

- The developed module by Mehboob *et al*. [14] was appropriate for early DR detection and protected the individuals from vision loss. However, it failed to offer the details about the severity of disease.
- The model was implemented by Bilal *et al*. [3], in dissimilar clinical setting, like remote or rural areas. But the method failed to improve the efficiency of classification by using ensemble learning schemes.

- DR is a medical state occurs on the individuals distressed from enduring diabetes. This causes vision loss due to the absence of early screening. Elevated sugar level in the blood is the major resource of DR. Manual recognition of DR is a tricky task because it influences the retinal region, leading to structural transformation.

3. Proposed Adaptive-RPO for Diabetic Retinopathy Detection

Diabetes is a chronic illness that arises due to the insufficient secretion of insulin by the pancreas. Over a period of time, this influenced the blood circulation system together with the retinal region. DR is a medicinal condition occurred because of the damage in retinal region and fluid leakage from blood vessels in the retina. Moreover, DR causes vision loss and the early screening by clinical experts is aided for avoiding blindness and other complications. To alleviate these problems, this paper presents an ARPO-based DCNN for diagnosing DR. At first, the input image is obtained from the specific database [23] and it is preprocessed with median filtering [11].

Table 1. Comparative discussion.

Reference	Research problem and significance	Methodology	Key findings and results	Contributions	Strengths	Weaknesses
Yaqoob *et al.* [34]	DR detection using optimized deep residual networks.	Deep residual network architecture with feature optimization.	Enhanced accuracy in detecting DR.	Development of an optimized deep residual network for detection.	High detection accuracy with optimized features.	Potential computational complexity.
Nazir *et al.* [21]	DR detection through hybrid feature extraction.	Hybrid feature extraction with SVM for classification.	Improved detection accuracy using hybrid features.	Integration of hybrid feature extraction with SVM.	Effective feature extraction and classification.	May not generalize well to all datasets.
Liu *et al.* [12]	Novel approach for detecting DR using symmetric CNN.	Deep symmetric CNN.	High detection accuracy with symmetric CNN.	Introduction of a novel symmetric CNN for detection.	High performance with innovative network design.	Computationally intensive.
Sharma *et al.* [28]	Improved pre-processing techniques for DR detection.	Machine learning with enhanced pre-processing methods.	Increased detection accuracy with better pre-processing.	Enhanced pre-processing techniques.	Improved detection with advanced pre-processing.	Dependent on pre-processing quality.
Hari *et al.* [7]	Detection of DR with enhanced features.	Feature enhancement with DL.	Improved detection accuracy through feature enhancement.	Use of feature enhancement techniques with DL.	High detection rates with enhanced features.	May require fine-tuning for different datasets.
Yazhini and Loganathan [35]	DR diagnosis using integrated fusion-based model.	Fusion-based feature extraction and classification model.	High accuracy in diagnosis using fusion techniques.	Integration of fusion techniques for improved diagnosis.	Accurate and robust diagnosis model.	Complexity in fusing multiple features.
Lahmar and Idri [9]	Detection of referable DR using deep features.	Deep feature extraction combined with random forest.	High accuracy in detecting referable DR.	Combination of DL with random forest.	Effective in detecting referable cases.	May require large datasets for training.
Mukherjee and Sengupta [16]	Detection and gradation of DR using hybrid CNN.	Hybrid CNN for deep feature extraction and classification.	Accurate detection and grading of DR.	Development of a hybrid CNN for robust feature extraction.	High performance in feature extraction and classification.	Complexity in CNN architecture design.
Ishtiaq *et al.* [8]	DR detection using hybrid ensemble-optimized CNN.	Ensemble-optimized CNN with texture feature extraction.	Improved detection accuracy using hybrid techniques.	Integration of CNN and texture features for enhanced detection.	Effective combination of CNN and texture features.	May require extensive computational resources.
Nahiduzzaman *et al.* [18]	DR identification using parallel CNN and Extreme Learning Machine (ELM).	Parallel CNN for feature extraction and ELM for classification.	High accuracy in identifying DR.	Parallel CNN approach for efficient feature extraction.	High performance in feature extraction and classification.	Complex parallel processing may increase computational load.
Mukherjee and Sengupta [17]	Comparison of deep feature extraction strategies for DR stage classification.	Comparative analysis of different deep feature extraction techniques.	Identification of the most effective feature extraction strategy.	Comprehensive comparison of multiple DL techniques.	Valuable insights into feature extraction strategies.	Results may vary depending on dataset characteristics.
Parthiban and Kamarasan [22]	Detection and grading of DR using coyote optimization.	Coyote optimization algorithm combined with DL.	Accurate detection and grading of DR.	Application of coyote optimization in DL for DR detection.	High accuracy in detection and grading.	Complexity in optimization and DL integration.
Saranya and Umamaheswari [26]	Detection of exudates for non-proliferative DR.	DL model for exudate detection.	High accuracy in detecting exudates from retinal images.	Application of DL for specific DR features.	Effective in detecting early signs of DR.	Limited to non-proliferative DR detection.
Malhi *et al.* [13]	Detection and grading of DR using digital retinal images.	Digital image processing and grading model.	Accurate grading of DR severity.	Use of digital image processing for DR grading.	Accurate grading with digital image analysis.	May require high-quality retinal images.
Vijayan *et al.* [32]	DR recognition using color histogram filter.	Feature selection based on color histogram filter.	Improved recognition accuracy using simple filters.	Development of a simple yet effective feature selection method.	Low computational complexity.	May not perform well with complex features.
Usman *et al.* [31]	Detection of DR using Principal Component Analysis (PCA) for multi-label feature extraction.	PCA for feature extraction and classification.	Accurate detection using multi-label feature extraction.	Application of PCA for multi-label DR detection.	Effective in reducing feature dimensionality.	May lose important information during PCA.
Navaneethan and Devarajan [20]	Enhanced detection of DR using Modified Generative Adversarial-based Crossover Salp Grasshopper (MGA-CSG) algorithm.	MGA-CSG algorithm for preprocessing and feature extraction.	Improved detection accuracy with enhanced preprocessing.	Introduction of a novel preprocessing algorithm for DR detection.	Effective in enhancing detection accuracy.	Complexity in algorithm design and implementation.

Then, lesion segmentation is executed using U-Net to segment the lesions into MAs, hard as well as soft exudates and haemorrhages [25]. Finally, the DCNN is utilized for detecting DR [24] by considering segmented image as well as the input image. Here, DCNN is trained by Adaptive-RPO, such that ARPO is modified using

adaptive concept with RPO [6]. Figure 1 shows the illustration of ARPO-based DCNN for the detection of DR.

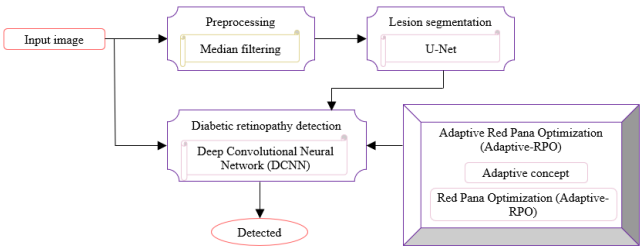

Figure 1. Block diagram for ARPO-based DCNN, DR detection.

3.1. Image Acquisition

A traditional IDRiD is considered with amount of sample images. The expression of initialization process is given by,

$$Y = \{Y_1, Y_2, \ldots Y_f \ldots Y_h\} \tag{1}$$

Where Y implies the input database, h refers the total amount of retinal image samples, in which Y_f is used for detecting DR.

3.2. Image Preprocessing with Median Filter

Image preprocessing is used for enhancing the quality of images before the operation of detection tasks. In this approach, median filter preprocesses the input image, as this replaces the value of pixel in an image with the median rate of its neighboring pixels by preserving the edges of image while smoothing out unwanted variations in pixel intensity. The median filter [11] is the well-organized nonlinear filter and it performs effectual removal of redundancies. The term of median filter is specified as,

$$\hat{A}(x,y) = \text{Med}_{(p,q)\in W_{xy}}\{Y_f\} \tag{2}$$

Where Y_f represents the input data. The accomplished preprocessed image is indicated as.

The application of the median filter as a preprocessing step is critical for enhancing the quality of retinal fundus images prior to subsequent segmentation and classification. The median filter effectively suppresses impulse noise while preserving important edge information, which is essential for accurate delineation of retinal lesions. This preservation of structural details directly contributes to improved segmentation outcomes and, consequently, more reliable DR detection. Compared to other common preprocessing techniques such as mean or Gaussian filtering, the median filter is particularly advantageous in medical imaging because it reduces noise without introducing significant blurring, thereby maintaining the integrity of fine anatomical features. Although guided filters are also recognized for their edge-preserving properties and have been explored in retinal image enhancement, they typically involve higher computational complexity and parameter tuning, which may not yield substantial benefits for the specific noise characteristics present in the IDRiD dataset. The choice of the median filter in this study is thus motivated by its balance of simplicity, effectiveness, and its proven ability to enhance image quality for robust downstream analysis.

3.3. Lesion Segmentation with U-Net

Lesion segmentation performs the automated detection of outline areas of interest within the images and provides precise and reliable information about the location, size, and characteristics of lesions. This approach identifies abnormal lesions from the given preprocessed image P_f. Here, the lesions are segmented by the utilization of U-Net [25, 29]. This network contains contracting path, as well as expanding path. The contracting path includes the generic structure of CNN with convolution, max pooling and activation functions. Likewise, the expanding path up samples the feature map and perform cropping and concatenation. Finally, the convolution function is emerged for minimizing the feature map size. The energy function of the U-Net is taken as,

$$E_U = \sum_{d\in K} C(d) log\big(Q_{J(d)}(d)\big) \tag{3}$$

Where Q_J represents Softmax function applied over the feature map, this function is specified as,

$$Q_J = EXP\big(s_J(d)\big) / \sum_{g=1}^{E} EXP\big(s_J(d)'\big) \tag{4}$$

Where s_J represents the activation function of channel J. The accomplished segmented image from the U-Net is specified as U_f. Figure 2 shows the structural design of U-Net.

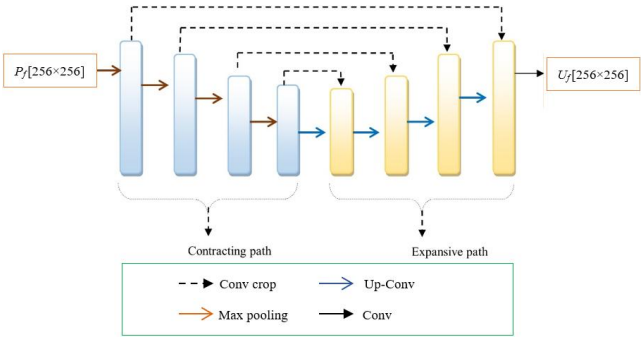

Figure 2. Structure of U-Net.

U-Net is widely preferred for medical image segmentation tasks, including DR lesion segmentation, due to several key advantages over other architectures. Its encoder-decoder structure with skip connections enables the network to capture both global context and fine-grained spatial details, which is critical for accurately delineating small and scattered lesions in fundus images. The skip connections help preserve high-resolution features that might otherwise be lost

during down-sampling, resulting in more precise segmentation boundaries. Additionally, U-Net performs well even with limited annotated data, a common scenario in medical imaging, thanks to its efficient use of data augmentation and fully convolutional design. Compared to other models such as Fully Convolutional Network (FCN) or SegNet, U-Net consistently achieves higher segmentation accuracy and better delineation of lesion boundaries in DR datasets. These characteristics make U-Net particularly well-suited for the precise and reliable segmentation required in automated DR detection.

3.4. DCNN for Detecting Diabetic Retinopathy

In this phase, the input R_f is subjected to the DCNN for DR detection. Such that $R_f \in \{U_f, Y_f\}$; here U_f represents segmented image and Y_f denotes the input image. By leveraging the hierarchical structure of CNNs, these networks automatically capture both low-level and high-level features and extract intricate features from the segmented fundus image.

3.4.1. Structure of DCNN

The multi-layered architecture of CNNs [24] enables them to discern subtle patterns and variations in the input R_f for early detection of DR disease. Initially, the input R_f is given to the first layer. Here, convolution layer contains dissimilar kernel size and convolution strides for feature extraction and the pooling layer is integrated for sampling the feature maps. Furthermore, the FC layer is a classifier and it is presented in the final stage of the network. The layers of the DCNN are explained below,

a) Convolutional layer: this layer is featuring extractors, and it has an ability to learn the feature representations of real image images. The presented neurons in the layer are grouped as feature maps. The accomplished final feature map is formulated by,

$$a_\alpha = H(G_\alpha * R_f) \tag{5}$$

Where a_α denotes the resulting feature map, R_f implies the input image, $H(.)$ represents the nonlinear activation function, and G_α indicates the convolution filter.

b) Pooling layer: this layer is employed to moderate the spatial solution of feature maps. Therefore, it accomplishes spatial invariance to input distortions. The selection of larger elements is conducted in this layer based on the following expression,

$$a_{\alpha(p,q)} = \underset{(x,y)\in\rho_{pq}}{MAX} R_f(x,y) \tag{6}$$

Where ρ_{pq} specifies the pooling region, $a_{\alpha(p,\ q)}$ and $R_f(x, y)$ represents the elements in region (x, y).

c) Fully Connected (FC) layer: the FC layer interprets the feature representations and performs the function of high-level reasoning. The achieved detected result from the DCNN architecture is specified by D_f. Figure 3 displays the graphical representation of DCNN.

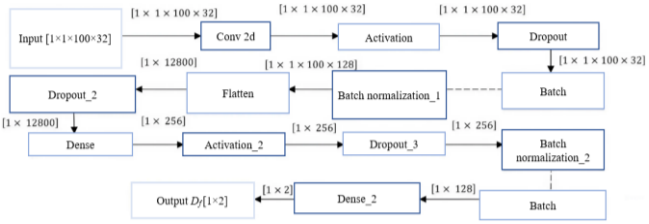

Figure 3. The structural design of DCNN.

3.4.2. ARPO for Training the DCNN

This part details the employed ARPO for tuning the DCNN. Here, the APRO is employed by combining RPO and Adaptive concept with the inspiration of the activities of red panda. Moreover, the food searching and sleeping behaviors are clever actions that have an ability to develop a global optimization. The arithmetical modeling of ARPO is explained below.

a) Solution Ancoding

The main goal of this process is to accomplish optimum decision in an exploration space with size I, such that and $I \in [1\times\zeta]$ is the learning measure of DCNN.

b) Fitness Function

The fitness is determined for accomplishing better solution in the searching area. The expression of fitness function is given by,

$$U_{Fit} = \frac{1}{f}\sum_{h=1}^{f}[\eta - D_f]^2 \tag{7}$$

Where h refers the total samples, f refers the range of η samples, specifies the target feature and D_f represents the output of DCNN. The algorithmic flow of ARPO is explained below,

- *Step* 1: Initialization.

In RPO, the members in the population are a number of red pandas. The population of panda in the specific search space is initialized as follows,

$$P = \{P_1, P_2, \ldots, P_l, \ldots, P_o\} \tag{8}$$

Where P refers the population of red panda, and P_l represents the l^{th} red panda utilized for the exploration of RPO.

- *Step* 2: Fitness function.

The fitness is served as a quantifiable measure of how well a solution is utilized for achieving the desired objective function. Here, the fitness is determined with Equation (7).

- *Step* 3: Exploration phase.

The location of pandas is modeled through its foraging strategy. Here, the position is randomly calculated based

on the location of food position selected by the optimum panda.

$$T = \{Z_T | T \in \{1, 2, \dots, o\} \; and \; L_T < L_l\} \cup \{Z_{opt}\} \quad (9)$$

Where T_{iu} indicates the determined food source for red panda l and Z_{opt} is the location of panda for optimum resolution.

Subsequently, the location of panda is updated as follows,

$$Z_l^{T_1}: z_{l,v}^{T_1} = z_{l,v} + V \cdot (I_{l,v} - E \cdot z_{l,v}) \quad (10)$$

Where V is made adaptive and the expression of V based on adaptive concept is given by,

$$V = \frac{\left(C_{up}(v) - C_{low}(v)\right) \cdot \Psi}{Z} \quad (11)$$

Where, Z refers the maximum iteration count, $C_{up}(v)$, $C_{low}(v)$ represents the upper and lower boundaries of problem variable v, Ψ, specifies the random number selected from set $\{1, 2\}$.

$$Z_l = \begin{cases} Z_l^{T_1}, & P_l^{T_1} < P_l \\ Z_l, & Otherwise \end{cases} \quad (12)$$

Where $Z_l^{T_1}$ indicates the new location of l^{th} panda,

- *Step* 4: Exploitation phase.

The behavior of pandas in climbing trees is modeled based upon the following attributes. Initially, a new space of each panda is determined. After that, the objective function is enhanced and the previous area of panda is replaced. The mathematical modeling of above process is given as follows,

$$z_{l,v}^{T_2} = z_{l,v} \frac{\left(C_{low}(v) + V \cdot (C_{up}(v) - C_{low}(v)\right)}{Z}, l = 1,2,..o, v = 1,2,..g, Z = 1,2,..y \quad (13)$$

$$Z_l = \begin{cases} Z_l^{T_2}, & P_l^{T_2} < P_l \\ Z_l, & Otherwise \end{cases} \quad (14)$$

Where $Z_l^{T_2}$ indicates the new location of the red panda l, $P_l^{T_2}$ refers the relative objective function. Algorithm (1) demonstrates the pseudo code of ARPO.

- Step 5: Re-evaluation of fitness function.

The Fitness of the above execution is recalculated to attain optimal result in the search space by using Equation (7).

- Step 6: Termination.

The above procedure is iteratively executed till achieving the finest decision. Algorithm (1) represents the pseudo code of ARPO.

Algorithm 1: Pseudo code of ARPO.

Input: $Z_l^{T_1}$
Output: $Z_{l,v}^{T_2}$
Initialize the populace P
For l=1 *to o*
Determine objective function using Equation (7)
Exploration phase: Update the location of l^{th} red panda based on first phase using Equation (11)
Determine the position of panda using Equation (12)
Exploitation phase: Update the area of l^{th} panda based on second stage using Equation (13)
Determine the location of panda using Equation (14)
End For
Termination

4. Result and Discussion

The performance of ARPO-based DCNN is evaluated in this part. Here, the evaluation of devised module is performed on the experimental settings along with the effectiveness of ARPO-based DCNN is validated with its conventional systems for revealing its effectiveness. This study utilizes the publicly available IDRiD, which comprises a total of 516 high-resolution retinal fundus images. The dataset is divided into 413 images for training and 103 images for testing, with each image annotated for DR severity as well as specific lesion types, including microaneurysms, HEs, hard exudates, and soft exudates. All images are provided at a resolution of 4288×2848 pixels, ensuring the preservation of fine anatomical details necessary for accurate analysis. Prior to model training, each image underwent preprocessing with a median filter to suppress noise while retaining essential edge information, followed by resizing to a standardized dimension suitable for the DL models. To improve model robustness and address potential class imbalance, data augmentation techniques such as random rotations, horizontal and vertical flipping, and brightness adjustments were applied during training. These steps collectively enhance the reproducibility of the study and provide a comprehensive foundation for the reported results.

4.1. Experimental Setup

The ARPO-based DCNN for detecting DR is tested in Python with Personal Computer (PC) that contains Windows 10-Operating System (OS).

4.2. Dataset Description

The IDRiD [23] constitutes classic DR lesions and standard structure of eye annotated at a pixel range. This database offers information about DR severity, and macular edema for all retinal images.

4.3. Experimental Outcomes

Figure 4 demonstrates the stepwise outcomes of the proposed ARPO-based DCNN approach. The original fundus Figure 4-a) and (b) are initially preprocessed using a median filter to enhance image quality and suppress noise, as shown in Figure 4-c) and (d). Subsequent lesion segmentation using U-Net yields the segmented in Figure 4-e) and (f), highlighting the

effectiveness of the proposed method in accurately isolating relevant retinal features. These results illustrate the capability of the ARPO-based DCNN to process raw fundus images and produce clear, clinically meaningful segmentations, which are essential for reliable DR detection.

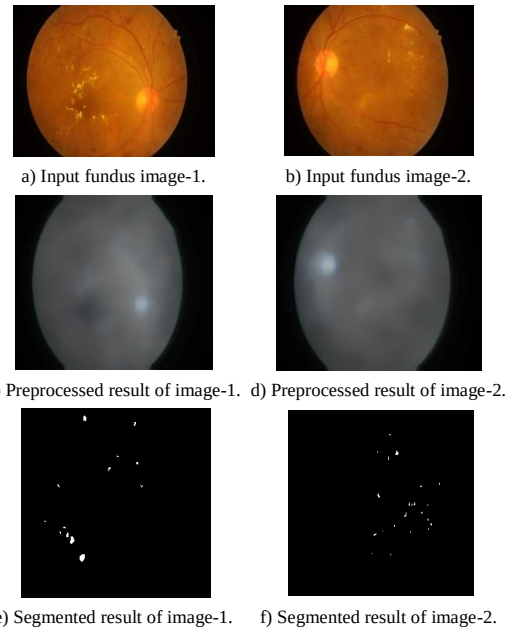

a) Input fundus image-1. b) Input fundus image-2.

c) Preprocessed result of image-1. d) Preprocessed result of image-2.

e) Segmented result of image-1. f) Segmented result of image-2.

Figure 4. Experimental outcomes of the ARPO-based DCNN.

4.4. Evaluation Metrics

The significant performance metrics used for the validation of presented model is deliberated in this part. To ensure a comprehensive and clinically meaningful assessment of the model's performance, this study employs key evaluation metrics including accuracy, sensitivity, and specificity. Accuracy reflects the overall proportion of correctly classified cases, providing a general measure of the model's predictive capability. Sensitivity, also known as the true positive rate, evaluates the model's ability to correctly identify cases of DR, while specificity measures the ability to correctly recognize non-diseased cases. By reporting these established metrics, the evaluation of the proposed DR detection framework remains robust, transparent, and directly relevant to clinical diagnostic standards.

The evaluation of DR detection performance is based on accuracy, sensitivity, and specificity, which are regarded as the most clinically relevant and widely accepted metrics in both medical and machine learning communities. These measures provide a clear and direct assessment of diagnostic capability and facilitate straightforward interpretation by healthcare practitioners. Although additional metrics such as Area Under the Curve-Receiver Operating Characteristic (AUC-ROC) and F1-score can offer further analytical perspectives, the focus on accuracy, sensitivity, and specificity ensures alignment with established clinical standards and supports transparent comparison with existing literature. Inclusion of supplementary metrics may be considered in future research to enable a more comprehensive evaluation framework.

4.4.1. Accuracy

Accuracy [19] is typically deliberated as the range of exact categorization DR disease among entire cases. This is measured using the following expression,

$$k_1 = \frac{L_\delta + S_\gamma}{L_\delta + L_\gamma + S_\delta + S_\gamma} \tag{15}$$

Where L_δ, L_y denotes true positive and negative, and S_δ, S_y indicates false positive and negative.

4.4.2. Sensitivity

Sensitivity [19] represents the proportion of true positive cases from total number of patients with DR disease. The calculation of sensitivity is done by,

$$k_2 = \frac{L_\delta}{L_\delta + S_\gamma} \tag{16}$$

4.4.3. Specificity

The percentage of true negative results among the total amount of patients who do not have DR is referred as a specificity [19]. The expression of specificity is given by,

$$k_3 = \frac{L_\gamma}{L_\gamma + S_\delta} \tag{17}$$

4.5. Comparative Methods

The assessment of ARPO-based DCNN is carried out to reveal the efficiency of the presented DR detection model. Herein, the classical detection schemes, such as Shark Smell-Jaya Optimization with Convolutional Neural Network-Long Short-Term Memory (SS-JO-CN-LSTM) [2], DNN [15], ResNet-101 [1], and VGGNet [3] are utilized for evaluation.

4.6. Comparative Evaluation

The evaluation of ARPO-based DCNN is explained in this part. The analysis of ARPO-based DCNN is conducted based on classical detection approaches with specified evaluation metrics.

4.6.1. Analysis of ARPO-Based DCNN with Training Data

Figure 5 displays the evaluation of ARPO-based DCNN with training data. Figure 5-a) exhibits the validation of ARPO-based DCNN based on accuracy. The ARPO-based DCNN attained accuracy as 90.278% and the typical models gained accuracy as 80.397%, 83.505%, 84.543%, and 87.555%. The improved efficiency obtained by the developed model is 10.945%, 7.502%, 6.353%, and 3.017% than its conventional detection modules. In Figure 5-b), the assessment of ARPO-based DCNN with sensitivity is exposed.

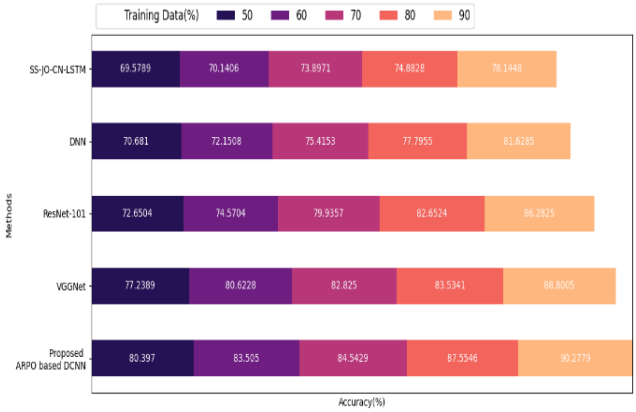

a) Accuracy.

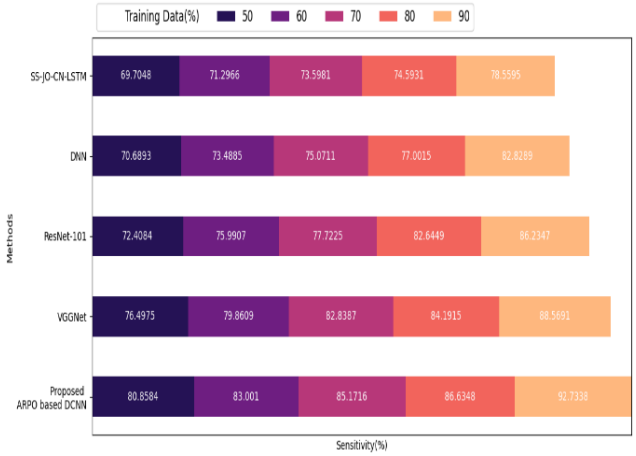

b) Sensitivity.

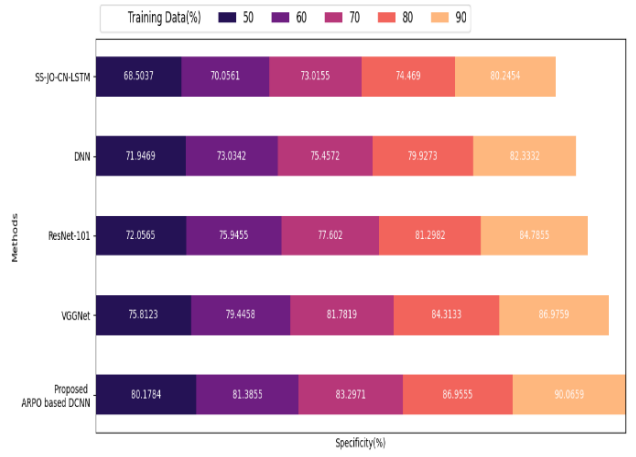

c) Specificity.

Figure 5. Assessment of ARPO-based DCNN.

The sensitivity accomplished by the devised model and its traditional schemes is 92.734%, 80.858%, 83.001%, 85.172%, and 86.635% while using training data=90%. The ARPO-based DCNN accomplished improved efficiency than its prior schemes as 12.806%, 10.495%, 8.155%, and 6.577%. Figure 5-c) displays the examination of ARPO-based DCNN with specificity. The specificity achieved by the presented module is 90.066% and its classical schemes attained specificity as 80.178%, 81.385%, 83.297%, and 86.956% with training data as 90%. The enhanced effectiveness gained by the developed method is 10.978%, 9.638%, 7.515%, as well as 3.453% than SS-JO-CN-LSTM, DNN, ResNet-101, and VGGNet.

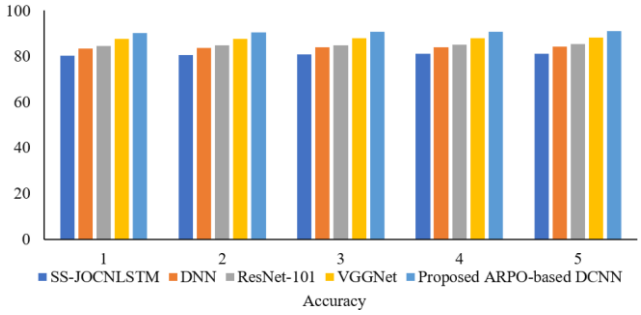

a) Accuracy.

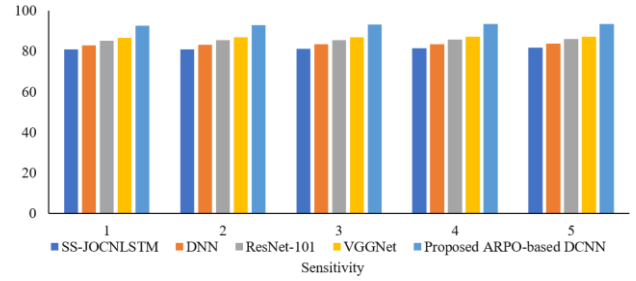

b) Sensitivity.

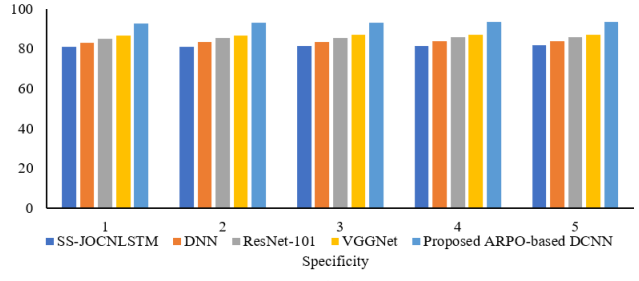

c) Specificity.

Figure 6. Assessment of ARPO-based DCNN for different epochs.

The analysis in Figure 6, of the ARPO-based DCNN with the training data demonstrates its superior performance across all evaluated Quality of Service (QoS) metrics-accuracy, sensitivity, and specificity-compared to SS-JO-CN-LSTM, DNN, ResNet-101, and VGGNet models over five epochs. In terms of accuracy, the ARPO-based DCNN consistently outperforms all other models, starting at 90.278% in the first epoch and progressively increasing to 91.1% in the fifth epoch. This improvement is notably higher than VGGNet, the second-best performer, which achieves a maximum accuracy of 88.15%, while ResNet-101, DNN, and SS-JO-CN-LSTM exhibit comparatively lower values, with SS-JO-CN-LSTM lagging the most. Similarly, the ARPO-based DCNN demonstrates exceptional sensitivity, increasing from 92.734% in the first epoch to 93.55% in the fifth epoch, indicating its robust ability to detect positive cases effectively. In contrast, VGGNet, ResNet-101, and other models show relatively lower sensitivity levels, with VGGNet achieving a maximum of 87.215%, emphasizing the superior generalization capability of the proposed model. Regarding specificity, the ARPO-based DCNN achieves the highest values, progressing from 90.066% to 90.87%, maintaining a significant margin over competing models, with VGGNet trailing at 87.535% by the final epoch. These results highlight the ARPO-

based DCNN's efficiency in minimizing false positives and ensuring precise classification. Overall, the consistent improvement across all metrics validates the effectiveness of the ARPO-based DCNN in handling complex training data and underscores its potential for practical deployment in real-world scenarios.

4.6.2. Analysis of ARPO-Based DCNN with K-Fold

Figure 7, illustrates the evaluation of ARPO-based DCNN with K-fold.

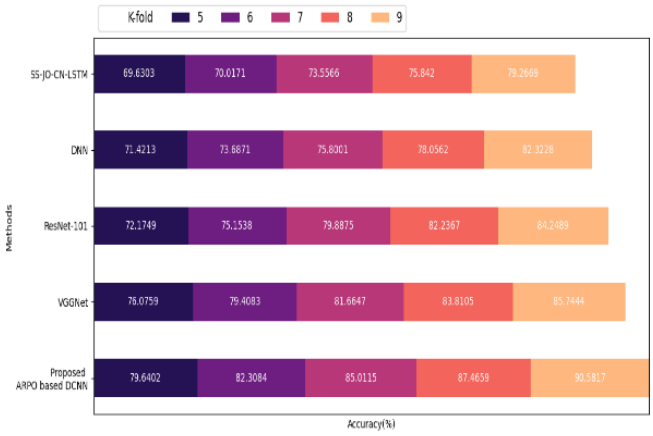

a) Accuracy.

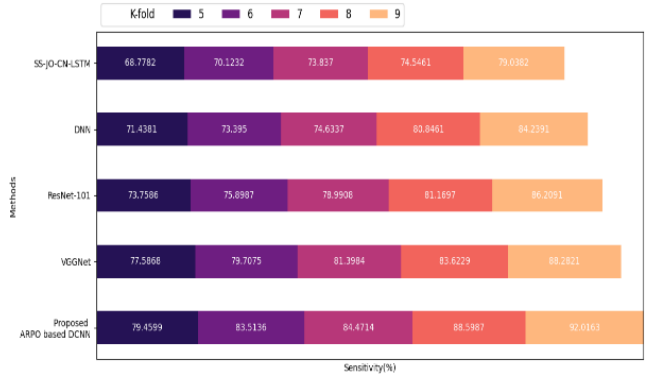

b) Sensitivity.

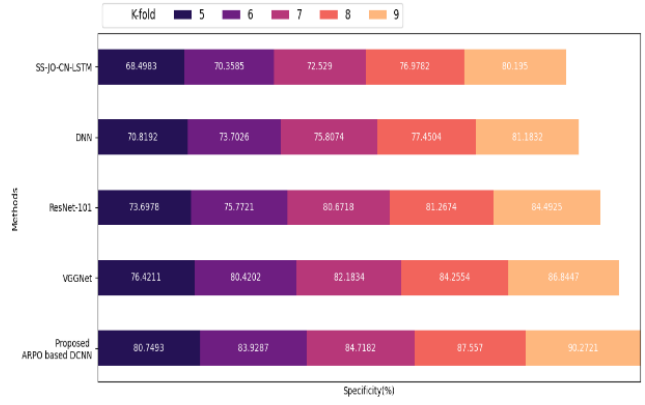

c) Specificity.

Figure 7. Analysis of ARPO-based DCNN.

In Figure 6-a), the evaluation of presented method with accuracy is displayed. The accuracy achieved by the presented scheme is 90.582% and the typical approaches achieved accuracy as 79.640%, 82.308%, 85.011%, and 87.466%. The superior performance gained by the developed approach is 12.079%, 9.133%, 6.149%, and 3.440% than its typical detection modules. In Figure 6-b), the validation of ARPO-based DCNN with sensitivity is illustrated. The sensitivity obtained by the devised model and its traditional model is 92.016%, 79.460%, 83.514%, 84.471%, and 88.599% with 90% of training data. The ARPO-based DCNN obtained improved efficiency than its prior schemes as 13.646%, 9.240%, 8.200%, and 3.714%. Figure 6-c) exhibits the evaluation of ARPO-based DCNN using specificity. The specificity achieved by the ARPO-based DCNN is 90.272% and its classical schemes attained specificity as 80.749%, 83.929%, 84.718%, and 87.557% using training data as 90%. The enhanced effectiveness conquered by the developed method is 10.549%, 7.027%, 6.152%, and 3.008% than SS-JO-CN-LSTM, DNN, ResNet-101, and VGGNet.

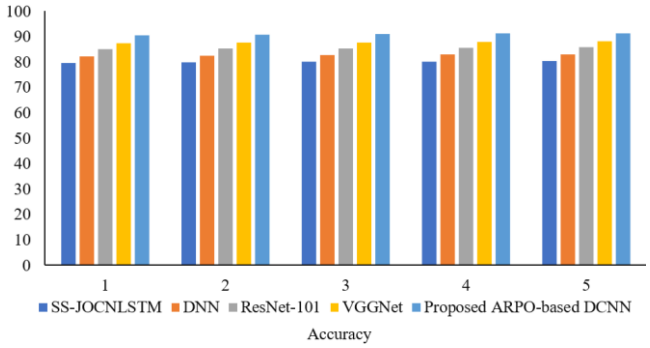

a) Accuracy.

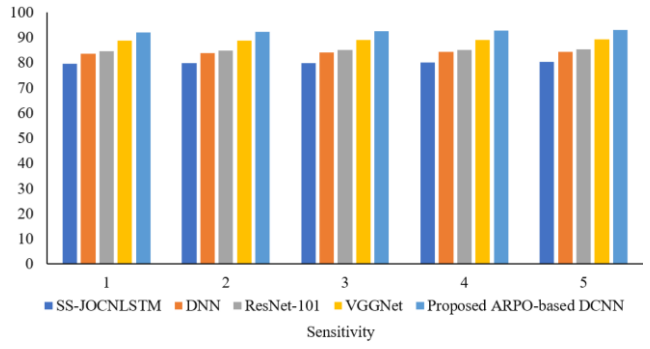

b) Sensitivity.

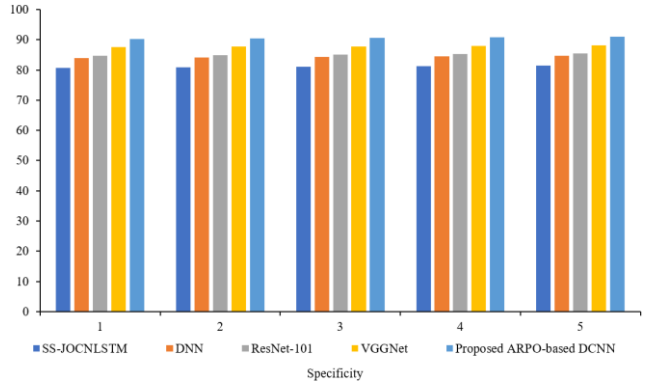

c) Specificity.

Figure 8. Analysis of ARPO-based DCNN for different epochs.

The performance analysis in Figure 8, of the ARPO-based DCNN with K-fold=9 cross-validation demonstrates its superior capability across all QoS metrics accuracy, sensitivity, and specificity-compared to SS-JO-CN-LSTM, DNN, ResNet-101, and VGGNet

over five epochs. In terms of accuracy, the ARPO-based DCNN starts with an impressive 90.582% in the first epoch and steadily increases to 91.4% by the fifth epoch, outperforming VGGNet, which achieves a maximum accuracy of 88.07%, and significantly surpassing ResNet-101, DNN, and SS-JO-CN-LSTM, which remain below 85.82%. This demonstrates the proposed model's superior learning capability and robustness. Regarding sensitivity, the ARPO-based DCNN consistently achieves the highest values, beginning at 92.016% in the first epoch and reaching 92.83% in the fifth epoch, reflecting its excellent ability to correctly identify positive cases. In contrast, VGGNet follows with a peak sensitivity of 89.2%, while ResNet-101 and other models display lower sensitivity values, highlighting their relatively reduced effectiveness in detecting positive instances. The specificity results further confirm the effectiveness of the ARPO-based DCNN, starting at 90.272% and increasing to 91.08% by the fifth epoch, indicating its strong ability to correctly identify negative cases with minimal false positives. This outperforms VGGNet, which attains a maximum specificity of 88.135%, while the remaining models lag behind, with SS-JO-CN-LSTM showing the lowest specificity values. The consistent improvements across all metrics reinforce the reliability and generalization capability of the ARPO-based DCNN, demonstrating its robustness in handling variations within the dataset under K-fold=9 validation, ensuring comprehensive model evaluation and improved real-world applicability.

4.7. Comparative Discussion

Table 2, reviews the evaluation results of ARPO-based DCNN. The accuracy attained by the presented model is 90.582% and the typical models achieved accuracy by 79.640%, 82.308%, 85.011%, and 87.466%. The achieved high accuracy makes the developed approach more accurate for early screening. The sensitivity achieved by the devised model and its traditional model is 92.016%, 79.460%, 83.514%, 84.471%, and 88.599%. This allows the system for the identification of greater true positive cases by reducing the risk of missing any potential instances of DR. The specificity attained by the ARPO-based DCNN is 90.272% and its classical schemes attained specificity as 80.749%, 83.929%, 84.718%, and 87.557%. The system with high specificity accurately distinguishes between DR and other retinal abnormalities. The assessment of ARPO-based DCNN attained accuracy, sensitivity and specificity as 90.582%, 92.016%, and 90.272% respectively.

Table 2. Comparative discussion using different QoS metrics.

Data	Methods/Metrics	SS-JO-CN-LSTM	DNN	ResNet-101	VGGNet	Proposed ARPO-based DCNN
Training data=90%	Accuracy (%)	80.397	83.505	84.543	87.555	90.278
	Sensitivity (%)	80.858	83.001	85.172	86.635	92.734
	Specificity (%)	80.178	81.385	83.297	86.956	90.066
K-fold=9	Accuracy (%)	79.640	82.308	85.011	87.466	90.582
	Sensitivity (%)	79.460	83.514	84.471	88.599	92.016
	Specificity (%)	80.749	83.929	84.718	87.557	90.272

Table 3. Comparative discussion on different epochs by considering the training Data=90%.

QoS Metric	Epochs	SS-JO-CN-LSTM	DNN	ResNet-101	VGGNet	Proposed ARPO-based DCNN
Accuracy (%)	1	80.397	83.505	84.543	87.555	90.278
	2	80.6	83.7	84.75	87.7	90.5
	3	80.8	83.9	84.95	87.85	90.7
	4	81	84.1	85.15	88	90.9
	5	81.2	84.3	85.35	88.15	91.1
Sensitivity (%)	1	80.858	83.001	85.172	86.635	92.734
	2	81.06	83.2	85.38	86.78	92.95
	3	81.26	83.4	85.58	86.925	93.15
	4	81.46	83.6	85.78	87.07	93.35
	5	81.66	83.8	85.98	87.215	93.55
Specificity (%)	1	80.178	81.385	83.297	86.956	90.066
	2	80.38	81.58	83.5	87.1	90.27
	3	80.58	81.78	83.7	87.245	90.47
	4	80.78	81.98	83.9	87.39	90.67
	5	80.98	82.18	84.1	87.535	90.87

The comparative analysis of the performance metrics presented in Table 3, demonstrates the superiority of the proposed ARPO-based DCNN model across all QoS metrics accuracy, sensitivity, and specificity compared to SS-JO-CN-LSTM, DNN, ResNet-101, and VGGNet. In terms of accuracy, the ARPO-based DCNN consistently outperforms other models, achieving the highest accuracy of 91.1% at the 5th epoch, which is significantly higher than the next best-performing model, VGGNet, at 88.15%, and far surpassing SS-JO-CN-LSTM at 81.2%. A similar trend is observed in sensitivity, where the proposed model achieves 93.55%, outperforming VGGNet (87.215%) and ResNet-101 (85.98%) at the 5th epoch, indicating its enhanced ability to correctly identify positive cases. Additionally, the ARPO-based DCNN achieves the highest specificity of 90.87%, reflecting its effectiveness in correctly identifying negative cases, compared to VGGNet at

87.535% and SS-JO-CN-LSTM at 80.98%. Across all epochs, the ARPO-based DCNN consistently demonstrates an increasing performance trend, highlighting its robustness and efficiency in improving classification outcomes over training iterations. The performance gap between the proposed model and existing architectures becomes more pronounced with additional epochs, affirming the effectiveness of the ARPO optimization technique in enhancing DL-based liver tumor classification.

Table 4. Comparative discussion on different epochs by considering the K-Fold=9.

QoS metric	Epochs	SS-JO-CN-LSTM	DNN	ResNet-101	VGGNet	Proposed ARPO-based DCNN
Accuracy (%)	1	79.64	82.308	85.011	87.466	90.582
	2	79.84	82.51	85.22	87.62	90.8
	3	80.04	82.71	85.42	87.77	91
	4	80.24	82.91	85.62	87.92	91.2
	5	80.44	83.11	85.82	88.07	91.4
Sensitivity (%)	1	79.46	83.514	84.471	88.599	92.016
	2	79.66	83.72	84.68	88.75	92.23
	3	79.86	83.92	84.88	88.9	92.43
	4	80.06	84.12	85.08	89.05	92.63
	5	80.26	84.32	85.28	89.2	92.83
Specificity (%)	1	80.749	83.929	84.718	87.557	90.272
	2	80.95	84.13	84.93	87.7	90.48
	3	81.15	84.33	85.13	87.845	90.68
	4	81.35	84.53	85.33	87.99	90.88
	5	81.55	84.73	85.53	88.135	91.08

The comparative analysis of the models presented in Table 4, reveals that the proposed ARPO-based DCNN consistently outperforms the other methods across all QoS metrics accuracy, sensitivity, and specificity over five epochs. In terms of accuracy, the ARPO-based DCNN achieves a steady increase from 90.582% in the first epoch to 91.4% in the fifth epoch, outperforming VGGNet, which follows as the second-best model with accuracy values ranging from 87.466% to 88.07%. Similarly, ResNet-101, DNN, and SS-JO-CN-LSTM demonstrate lower performance, with SS-JO-CN-LSTM achieving the least accuracy across all epochs. A similar trend is observed in sensitivity, where the ARPO-based DCNN shows the highest values, starting at 92.016% in the first epoch and reaching 92.83% by the fifth epoch, surpassing VGGNet's maximum sensitivity of 89.2%. ResNet-101 and DNN also demonstrate steady improvement but remain significantly lower than the proposed model. Regarding specificity, the ARPO-based DCNN consistently achieves the highest values, increasing from 90.272% to 91.08% across epochs, with VGGNet again being the second-best performer, followed by ResNet-101, DNN, and SS-JO-CN-LSTM. Overall, the superior performance of the ARPO-based DCNN across all QoS metrics highlights its effectiveness and robustness in comparison to conventional DL models.

While the proposed ARPO-based DCNN framework demonstrates strong diagnostic performance, it is important to acknowledge several limitations inherent to the approach. Firstly, the integration of deep convolutional layers, U-Net segmentation, and the adaptive optimization process contributes to considerable computational complexity. This increased complexity can lead to longer training times and necessitates access to high-performance computing resources, which may pose challenges for deployment in resource-limited clinical environments. Secondly, the effectiveness of the framework is sensitive to the quality and consistency of input fundus images. Variations in image quality due to noise, suboptimal illumination, or imaging artifacts can adversely impact both the segmentation and classification stages, potentially resulting in less reliable predictions. Furthermore, although the model achieves robust results on the IDRiD dataset, its generalizability to other datasets or real-world clinical settings may be affected by differences in imaging protocols or patient demographics. Addressing these limitations-such as by optimizing computational efficiency and incorporating advanced data augmentation or domain adaptation strategies-will be essential for facilitating broader clinical adoption in future work.

5. Conclusions

The early detection of DR moderates the serious complication of diabetes and offers timely treatment and prevents further progression of the disease and reduces the possibility of vision loss and complexities related to the disease, highlighting the importance of regular screening and monitoring for individuals with diabetes. However, the conventional detection approaches were limited by the inconsistencies in diagnosis and delays in treatment for patients with DR. To mitigate these issues, this study presents an ARPO-based DCNN for detecting DR disease. Firstly, the median filtering is utilized to preprocess the input fundus image. Afterward, the lesions are segmented with U-Net. At last, DR detection is done with DCNN by considering segmented image and the input image as input. Here, DCNN is trained with ARPO. The assessment of ARPO-based DCNN has obtained accuracy as 90.582%, sensitivity as 92.016% and specificity as 90.272%. In the future, the presented approach will be further enhanced by utilizing advanced hybrid neural networks to extract more detailed

information for the identification of subtle changes for the detection and classification of different stages of disease with even greater precision.

Acknowledgement

Authors acknowledge the support from Nagarjuna College Engineering and Technology for the facilities provided to carry out the research.

References

[1] Al-Omaisi A., Zhu C., Althubiti S., Al-Alimi D., and et al., "Detection of Diabetic Retinopathy in Retinal Fundus Images Using CNN Classification Models," *Electronics*, vol. 11, no. 17, pp. 1-20, 2022. https://doi.org/10.3390/electronics11172740

[2] Bansode B., Bakwad K., Dildar A., and Sable G., "Deep CNN-based Feature Extraction with Optimised LSTM for Enhanced Diabetic Retinopathy Detection," *Computer Methods in Biomechanics and Biomedical Engineering: Imaging and Visualization*, vol. 11, no. 3, pp. 960-975, 2023. https://doi.org/10.1080/21681163.2022.2124545

[3] Bilal A., Sun G., Mazhar S., Imran A., and Latif J., "A Transfer Learning and U-Net-based Automatic Detection of Diabetic Retinopathy from Fundus Images," *Computer Methods in Biomechanics and Biomedical Engineering: Imaging and Visualization*, vol. 10, no. 6, pp. 663-674, 2022. https://doi.org/10.1080/21681163.2021.2021111

[4] Butt M., Iskandar D., Abdelhamid S., Latif G., and Alghazo R., "Diabetic Retinopathy Detection from Fundus Images of the Eye Using Hybrid Deep Learning Features," *Diagnostics*, vol. 12, no. 7, pp. 1-17, 2022. DOI: 10.3390/diagnostics12071607

[5] Gandhimathi S. and Pillai K., "Detection of Neovascularization in Proliferative Diabetic Retinopathy Fundus Images," *The International Arab Journal of Information Technology*, vol. 15, no. 6, pp. 1000-1009, 2018. https://www.ccis2k.org/iajit/PDF/November%202018,%20No.%206/10816.pdf

[6] Givi H., Dehghani M., and Hubalovsky S., "Red Panda Optimization Algorithm: An Effective Bio-Inspired Metaheuristic Algorithm for Solving Engineering Optimization Problems," *IEEE Access*, vol. 11, pp. 57203-57227, 2023. DOI: 10.1109/ACCESS.2023.3283422

[7] Hari K., Karthikeyan B., Reddy M., and Seethalakshmi R., "Diabetic Retinopathy Detection with Feature Enhancement and Deep Learning," *in Proceedings of the International Conference on System, Computation, Automation and Networking*, Puducherry, pp. 1-5, 2021. DOI: 10.1109/ICSCAN53069.2021.9526438

[8] Ishtiaq U., Abdullah E., and Ishtiaque Z., "A Hybrid Technique for Diabetic Retinopathy Detection Based on Ensemble-Optimized CNN and Texture Features," *Diagnostics*, vol. 13, no. 10, pp. 1-21, 2023. https://doi.org/10.3390/diagnostics13101816

[9] Lahmar C. and Idri A., "Referable Diabetic Retinopathy Detection Using Deep Feature Extraction and Random Forest," *in Proceedings of the 15th International Joint Conference Communications in Computer and Information Science*, Virtual, pp. 415-433, 2023. https://doi.org/10.1007/978-3-031-38854-5_21

[10] Lalithadevi B. and Krishnaveni S., "Detection of Diabetic Retinopathy and Related Retinal Disorders Using Fundus Images Based on Deep Learning and Image Processing Techniques: A Comprehensive Review," *Concurrency and Computation: Practice and Experience*, vol. 34, no. 19, pp. e7032, 2022. https://doi.org/10.1002/cpe.7032

[11] Liu S., Ni H., Zhong Y., Yan W., and Wang W., "Adaptive Weighted Median Filtering for Time-Varying Graph Signals," *Signal, Image and Video Processing*, vol. 19, pp. 88, 2025. https://doi.org/10.1007/s11760-024-03610-6

[12] Liu T., Chen Y., Shen H., Zhou R., Zhang M., and Liu T., "A Novel Diabetic Retinopathy Detection Approach Based on Deep Symmetric Convolutional Neural Network," *IEEE Access*, vol. 9, pp. 160552-160558, 2021. DOI: 10.1109/ACCESS.2021.3131630

[13] Malhi A., Grewal R., and Pannu H., "Detection and Diabetic Retinopathy Grading Using Digital Retinal Images," *International Journal of Intelligent Robotics and Applications*, vol. 7, pp. 426-458, 2023. https://doi.org/10.1007/s41315-022-00269-5

[14] Mehboob A., Akram M., Alghamdi N., and Abdul Salam A., "A Deep Learning Based Approach for Grading of Diabetic Retinopathy Using Large Fundus Image Dataset," *Diagnostics*, vol. 12, no. 12, pp. 1-20, 2022. https://doi.org/10.3390/diagnostics12123084

[15] Mujeeb Rahman K., Nasor M., and Imran A., "Automatic Screening of Diabetic Retinopathy Using Fundus Images and Machine Learning Algorithms," *Diagnostics*, vol. 12, no. 9, pp. 1-18, 2022. https://doi.org/10.3390/diagnostics12092262

[16] Mukherjee N. and Sengupta S., "A Hybrid CNN Model for Deep Feature Extraction for Diabetic Retinopathy Detection and Gradation," *International Journal on Artificial Intelligence Tools*, vol. 32, no. 8, pp. 2350036, 2023. https://doi.org/10.1142/S0218213023500367

[17] Mukherjee N. and Sengupta S., "Comparing Deep

Feature Extraction Strategies for Diabetic Retinopathy Stage Classification from Fundus Images," *Arabian Journal for Science and Engineering*, vol. 48, no. 8, pp. 10335-10354, 2023. https://doi.org/10.1007/s13369-022-07547-1

[18] Nahiduzzaman, Islam R., Goni O., Anower S., Ahsan M., Haider J., and Kowalski M., "Diabetic Retinopathy Identification Using Parallel Convolutional Neural Network Based Feature Extractor and ELM Classifier," *Expert Systems with Applications*, vol. 217, pp. 119557, 2023. https://doi.org/10.1016/j.eswa.2023.119557

[19] Natarajan B., Elakkiya R., Bhuvaneswari R., Saleem K., Chaudhary D., and Samsudeen S., "Creating Alert Messages Based on Wild Animal Activity Detection Using Hybrid Deep Neural Networks," *IEEE Access*, vol. 11, pp. 67308-67321, 2023. DOI: 10.1109/ACCESS.2023.3289586

[20] Navaneethan R. and Devarajan H., "Enhancing Diabetic Retinopathy Detection through Preprocessing and Feature Extraction with MGA-CSG Algorithm," *Expert Systems with Applications*, vol. 249, pp. 123418, 2024. https://doi.org/10.1016/j.eswa.2024.123418

[21] Nazir T., Javed A., Masood M., Rashid J., and Kanwal S., "Diabetic Retinopathy Detection Based on Hybrid Feature Extraction and SVM," *in Proceedings of the 13th International Conference on Mathematics, Actuarial Science, Computer Science and Statistics*, Karachi, pp. 1-6, 2019. DOI: 10.1109/MACS48846.2019.9024812

[22] Parthiban K. and Kamarasan M., "Diabetic Retinopathy Detection and Grading of Retinal Fundus Images Using Coyote Optimization Algorithm with Deep Learning," *Multimedia Tools and Applications*, vol. 82, no. 12, pp. 18947-18966, 2022. https://doi.org/10.1007/s11042-022-14234-8

[23] Porwal P., Pachade S., Kamble R., Kokare M., and et al., Indian Diabetic Retinopathy Image Dataset, IEE Data Port, https://ieee-dataport.org/open-access/indian-diabetic-retinopathy-image-dataset-idrid, Last Visited, 2024.

[24] Rawat W. and Wang Z., "Deep Convolutional Neural Networks for Image Classification: A Comprehensive Review," *Neural Computation*, vol. 29, no. 9, pp. 2352-2449, 2017. DOI: 10.1162/neco_a_00990

[25] Ronneberger O., Fischer P., and Brox T., "U-Net: Convolutional Networks for Biomedical Image Segmentation," *in Proceedings of the 18th International Conference in Medical Image Computing and Computer-Assisted Intervention*, Munich, pp. 234-241, 2015. https://doi.org/10.1007/978-3-319-24574-4_28

[26] Saranya P. and Umamaheswari K., "Detection of Exudates from Retinal Images for Non-Proliferative Diabetic Retinopathy Detection Using Deep Learning Model," *Multimedia Tools and Applications*, vol. 83, no. 17, pp. 52253-52273, 2023. https://doi.org/10.1007/s11042-023-17462-8

[27] Saranya P., Prabakaran S., Kumar R., and Das E., "Blood Vessel Segmentation in Retinal Fundus Images for Proliferative Diabetic Retinopathy Screening Using Deep Learning," *The Visual Computer*, vol. 38, pp. 977-992, 2022. https://doi.org/10.1007/s00371-021-02062-0

[28] Sharma A., Shinde S., Shaikh I., Vyas M., and Rani S., "Machine Learning Approach for Detection of Diabetic Retinopathy with Improved Pre-Processing," *in Proceedings of the International Conference on Computing, Communication, and Intelligent Systems*, Greater Noida, pp. 517-522, 2021. DOI: 10.1109/ICCCIS51004.2021.9397115

[29] Siddique N., Paheding S., Elkin C., and Devabhaktuni V., "U-Net and its Variants for Medical Image Segmentation: A Review of Theory and Applications," *IEEE Access*, vol. 9, pp. 82031-82057, 2021. DOI: 10.1109/ACCESS.2021.3086020

[30] Sowmya B., Meeradevi., Alex S., Kanavalli A., and et al., "Machine Learning Model for Emotion Detection and Recognition Using an Enhanced Convolutional Neural Network," *Journal of Integrated Science and Technology*, vol. 12, no. 4, pp. 1-10, 2024. https://doi.org/10.62110/sciencein.jist.2024.v12.786

[31] Usman T., Saheed Y., Ignace D., and Nsang A., "Diabetic Retinopathy Detection Using Principal Component Analysis Multi-Label Feature Extraction and Classification," *International Journal of Cognitive Computing in Engineering*, vol. 4, pp. 78-88, 2023. https://doi.org/10.1016/j.ijcce.2023.02.002

[32] Vijayan T., Sangeetha M., Kumaravel A., and Karthik B., "Feature Selection for Simple Color Histogram Filter Based on Retinal Fundus Images for Diabetic Retinopathy Recognition," *IETE Journal of Research*, vol. 69, no. 2, pp. 987-994, 2023. https://doi.org/10.1080/03772063.2020.1844082

[33] Wan C., Chen Y., Li H., Zheng B., and et al., "EAD-Net: A Novel Lesion Segmentation Method in Diabetic Retinopathy Using Neural Networks," *Disease Markers*, vol. 2021, no. 1, pp. 1-13, 2021. https://doi.org/10.1155/2021/6482665

[34] Yaqoob M., Ali S., Kareem I., and Fraz M., "Feature-based Optimized Deep Residual Network Architecture for Diabetic Retinopathy Detection," *in Proceedings of the 23rd International Multitopic Conference*, Bahawalpur, pp. 1-6, 2020. DOI:

10.1109/INMIC50486.2020.9318096

[35] Yazhini K. and Loganathan D., "An Integrated Fusion Based Feature Extraction and Classification Model for Diabetic Retinopathy Diagnosis," *in Proceedings of the 2nd International Conference on Inventive Research in Computing Applications*, Coimbatore, pp. 1187-1193, 2020. DOI: 10.1109/ICIRCA48905.2020.9183240

Mahesh Ramakrishnappa completed his Bachelor of Engineering Degree in SJC Institute of Technology, Chickballapura from Visvesvaraya Technological University, Belgaum in the field of Electronics and Communication Engineering in 2009. He also completed Master of Engineering degree in the area of Electronics and Communication Engineering, UVCE, Bangalore affiliated to Bangalore University in 2012. He is pursuing his Ph.D. Degree in Visvesvaraya Technological University, Belgaum in the area of Image Processing. He has 13 years of teaching experience and currently working as Assistant Professor in Department of Electronics and Communication, Nagarjuna College of Engineering and Technology, Bengaluru.

Rohith Shivashankar completed his Bachelor of Engineering degree in Nagarjuna College of Engineering and Technology, Bangaluru from Visvesvaraya Technological University, Belgaum in the field of Electronics and Communication Engineering in 2006. He also completed Master of Technology degree in the area of VLSI Design and Embedded systems in Dr. Ambedkar Institute of technology, Bangalore affiliated Visvesvaraya Technological University, Belgaum in 2008. He is also completed his Ph.D. degree from Visvesvaraya Technological University, Belgaum in the area of Digital Image Watermarking in 2020. He has 14 years of teaching experience and 1 year of industry experience and currently working as Associate Professor in Department of Electronics and Communication, NCET, Bangalore. He is working towards in the thrust research area such as Image processing, Cryptography, Information Hiding, VLSI design etc.